Available online at www.sciencedirect.com
ScienceDirect
Journal of Nuclear Materials 363–365 (2007) 1104–1109
journal of nuclear materials
www.elsevier.com/locate/jnucmat

Radiation distributions in TCV

G. Veres [a,*], R.A. Pitts [b], M. Wischmeier [c], B. Gulejova [b], J. Horacek [b], S. Kálvin [a]

[a] KFKI-RMKI, Research Institute for Particle and Nuclear Physics, EURATOM-Association, P.O. Box 49, H-1525 Budapest, Hungary
[b] CRPP-EPFL, Association EURATOM-Confédération Suisse, CH-1015 Lausanne, Switzerland
[c] Max-Planck-Institut für Plasmaphysik, EURATOM-Association, Boltzmann Str. 2., D-85748 Garching, Germany

Abstract

Total radiative powers measured by foil bolometer and AXUV camera systems are compared to SOLPS5 simulations in low and high density deuterium and helium diverted discharges on the TCV tokamak. For low density the match between simulation and measurements is satisfactory, but at high density strongly radiating regions outside the SOLPS5 simulation grid are seen in measurements and this may indicate the presence of enhanced convective particle transport in the low field side midplane region. The chord coverage of the foil bolometer system does not, however, allow detailed resolution in this region. The comparison of foil and AXUV data also demonstrates that ageing of the AXUV diodes under plasma irradiation combined with the unevenness of the diode spectral response, strongly limits their application for total radiative power measurements.

PACS: 52.25; 52.40; 52.70

Keywords: Divertor plasma; Impurity sources; Power balance; Radiation; TCV

1. Introduction

Measurement of total radiation profiles from tokamak plasmas is traditionally accomplished using tomographic inversion of the signals from bolometric cameras [1]. Such systems are sensitive to radiation from both photonic and from neutral particles. They are relatively slow, with time constants in the millisecond range and can be difficult to interpret in some circumstances, particularly in X-point configurations at high density, when neutral densities are high and the basic assumption of tomography (that the plasma be transparent to all the measured radiation) cannot always be satisfied. An alternative technique is to employ linear photodiode arrays which have recently seen increasing use [2–4]. These have the advantage of being considerably faster than foil bolometers (with time constants in the μs range) and are insensitive to neutrals. However, such diodes have a thin (typically 3–7 nm SiO_2) surface passivation layer, acting as an entrance window and reducing spectral responsivity in the low energy region (few 10's eV, see Fig. 1) where a significant fraction of radiation – especially in the edge/SOL and divertors of carbon dominated machines such as TCV where much of the radiation originates [5]. In addition to this variable spectral

* Corresponding author. Fax: +36 1 3922598.
E-mail address: veres@rmki.kfki.hu (G. Veres).

0022-3115/$ - see front matter © 2007 Elsevier B.V. All rights reserved.
doi:10.1016/j.jnucmat.2007.01.172

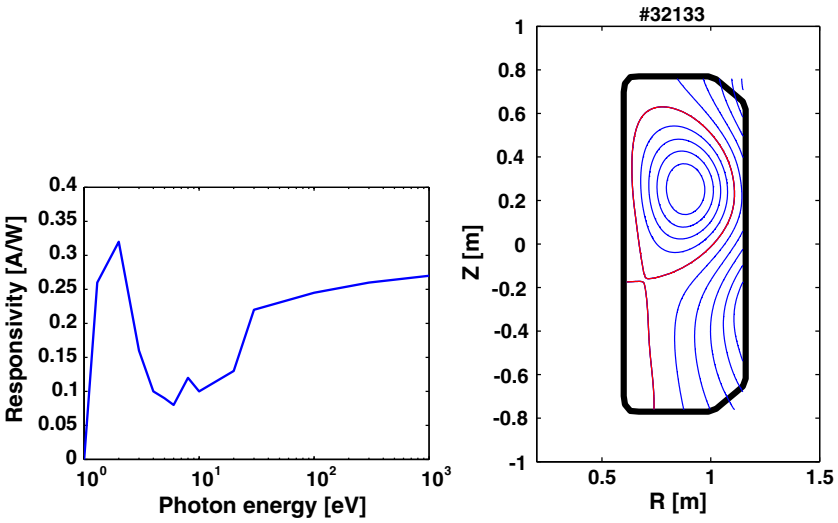

Fig. 1. Responsivity of the AXUV diodes and the magnetic configuration of our SNL plasmas.

response, AXUV diodes have another difficulty when in operation over many years on a tokamak: under plasma light irradiation the responsivity reduces further in precisely the same spectral range where the response is already reduced. To overcome this obstacle, regular calibration against a standard light source would be required in the 10–100 eV range (where no commonly available sources exist) or the diodes must be replaced at regular intervals. Alternatively, 'radiation hardened' diodes can be used (the TCV diodes are the standard AXUV EL detectors available from IRD [6]), but these are not readily available in compact, multi-detector form, as required for tomographic purposes.

Accounting for the non-flat AXUV spectral response in TCV (where much of the radiation in most cases of interest originates from low ionization states of carbon at low energies) is not possible without a complete model for the impurity production, transport and radiation. At first a primarily experimental study has thus been attempted, using low and high density ohmic plasmas in divertor configurations with deuterium and pure helium fuel species.

Helium plasmas have the attractive property of reduced charge-exchange neutral outfluxes and greatly reduced carbon concentrations, especially at high density, when a cold edge reduces physical sputtering of carbon in a regime in which carbon chemical sputtering is also largely absent (He is chemically inert and any chemical release is due to residual deuterium released from the walls). Helium has intense spectral lines in the same low energy spectral range where carbon species radiate strongly, but the power released over those helium spectral lines is considerably lower for helium, than for carbon (see e.g. the ADAS database [7]). The portion in the total measured radiated power falling in the non-flat AXUV diode spectral response is therefore expected to be reduced in He plasmas with lower carbon concentrations.

2. Experimental setup

The TCV tokamak has been equipped for many years with a 5 camera, 64 channel foil bolometer diagnostic [8], covering the entire vessel cross-section at a single toroidal location. Recently, a new 7 camera, 140 chord AXUV system has been installed in a common sector toroidally displaced by 90° from the foil bolometers [9].

The results presented here were obtained in matched He and D single null lower, ohmic diverted plasmas (see Fig. 1) with plasma current of 340 kA. In addition to fuel species, the plasma density, $\bar{n}_e$ has also been varied either in the form of a density ramp up to values approaching the density limit in a single discharge ($\bar{n}_e \sim 3 \rightarrow 12 \times 10^{19}$ m^{-3}) or in pulses with fixed density. The plasmas have $q_{95} \sim 3.5$ and triangularity, $\delta_{95} \sim 0.35$ for elongation $\kappa_{95} \sim 1.6$. Arrays of target embedded Langmuir probes are used to measure the power conducted and convected to the divertors and hence provide a check of overall power balance by comparison with total ohmic input and radiated power.

Tomographic reconstructions of foil bolometer and AXUV diode signals were obtained with serial

expansion constrained optimization with regularization using local base functions [10]. Based on these reconstructed profiles, the time dependence of the total radiative power emitted by the plasma was determined as well as the radiation emitted in different plasma regions.

3. Results and discussion

Fig. 2 shows the time variation in low density D and He plasmas of the plasma effective charge estimated from the distribution of soft X-ray radiation measured by a separate tomographic array of cameras [10].

Following the establishment of the full divertor configuration (at around 0.43 s), $Z_{\mathrm{eff}} \sim 1.2$ in D and about 2 in He, indicating low impurity concentrations in the plasma core. The time evolution of power balances for the two cases are illustrated in Fig. 2, where the ohmic input, is compared with the sum of the Langmuir probe (P_{SOL}) and radiative (P_{RAD}) powers. Extremely good balance is obtained ($P_{\Omega} = P_{\mathrm{SOL}} + P_{\mathrm{RAD}}$) only if the foil bolometer radiated power is assumed as the main radiative contribution – the AXUV system grossly underestimates the total by using the current-to-power conversion factor recommended in [2].

Interestingly, the AXUV power time evolution qualitatively matches that of the Z_{eff} – a rather surprising result, suggesting that the AXUV diodes pick up radiation mostly from the confined plasma region (from which the X-ray Z_{eff} is defined). These observation indicate at least two possible effects at play in determining the radiation fractions: the foil bolometry power (at least at low density) is negligibly influenced by any neutral contribution, and that the AXUV diodes (as a consequence of the reduced response at low energies and the ageing effect) are not enough sensitive to the low energy edge radiation for them to be of use in estimating the total power.

Fig. 3 shows the power balances for the high density deuterium and helium discharges. In these cases clearly $P_{\Omega} < P_{\mathrm{SOL}} + P_{\mathrm{RAD}}$, which discrepancy might have two origins: first, P_{RAD} is influenced by the neutral radiation, and second, the probes likely grossly overestimate the T_{e} (especially on the outer target) and hence the power. In the case of the deuterium discharge, the foil bolometry power is more than 50% of the Ohmic input, whereas in the helium discharge P_{RAD} is only about 30% of the Ohmic input at comparable AXUV (core radiation) powers.

The poloidal radiation distributions provided by the tomographic reconstruction provide an excellent experimental benchmark by which to test the results of edge code simulations of the TCV SOL. Such simulations have recently been performed using the SOLPS5 (B2.5-Eirene) code package [11] for He and D plasmas in precisely the discharge configuration used here [13,12]. Due to the low densities and the small (radial) sizes of the TCV divertor

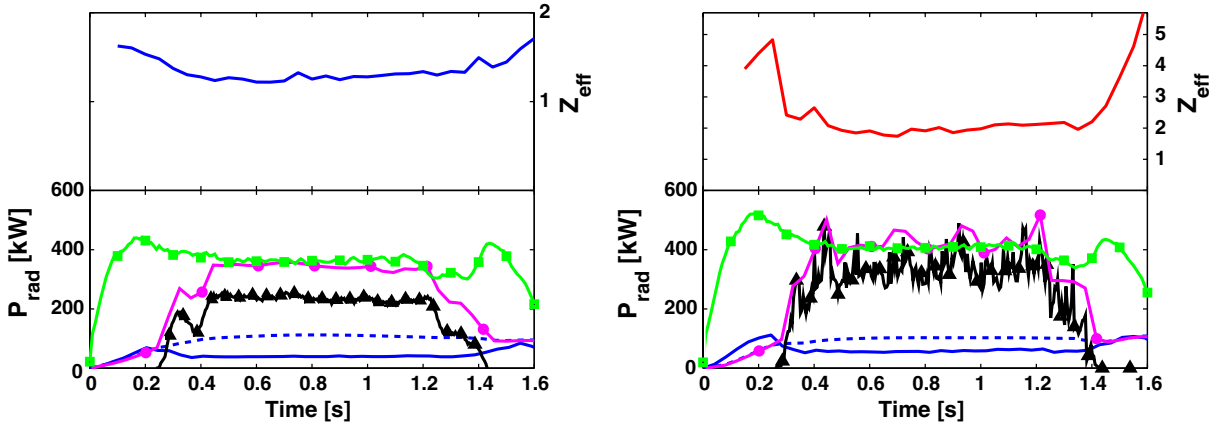

Fig. 2. Upper panels – The plasma effective charge for low density D discharge #32133 and low density He discharge #32138, respectively. Lower panels – Total radiative powers measured by the foil bolometers (dashed blue line) and AXUV diodes (solid blue line), the power reaching the divertor targets measured by Langmuir probes (black line), the Ohmic input power (green line) and the sum of the foil bolometer power and divertor target power (magenta line). (For interpretation of the references in color in this figure legend, the reader is referred to the web version of this article.)

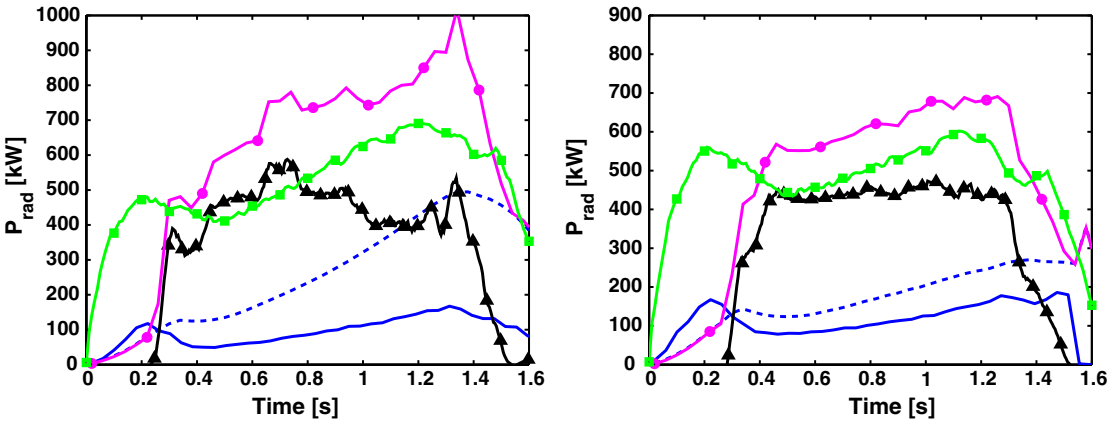

Fig. 3. Same as for Fig. 2, but for the high density D discharge #30319 (left figure) and high density He discharge #30337 (right figure).

and SOL plasmas no re-absorbtion or photo-ionization was taken into account in any of the radiation rates used in the simulations.

To compare code with experiment, the measured total radiative powers have been integrated over three specific regions: (1) – the area corresponding exactly to that covered by the SOLPS5 simulation grid (comprising all flux surfaces located 3 cm inside the midplane separatrix to 1.8 cm beyond it into the SOL) (2) – the region not covered by SOLPS5 inside the separatrix (i.e. comprising the flux surfaces located at more than 3 cm inside the midplane separatrix), and (3) – the region not covered by SOLPS5 outside the separatrix (i.e. located at more than 1.8 cm beyond the separatrix). Figs. 4 and 5 plot these three regions separated by flux surfaces shown by white lines.

A common feature of all Figs. 4 and 5 is that the SOLPS5 simulation predicts higher radiation than derived from the foil bolometers around the top high field side of the plasma at all densities studied. The origin of this discrepancy can be traced to a temperature drop (in the code simulation) in the vicinity of the upper X-point (located outside the vacuum vessel in this configuration). The code assumes impurities to be evenly eroded from all plasma-facing surfaces and this, combined with the low temperatures and long residence times of low charge state ionized impurities near the second X-point, provides for the high predicted radiation. Such trends are evidently not observed experimentally – except a slight radiation increase in that region in the high density He discharge, Fig. 5, pointing to an inaccurate description of the impurity production in this region.

Whilst the code predicts a radiation source where none is found experimentally, the foil bolometry reconstructions clearly show enhanced radiation

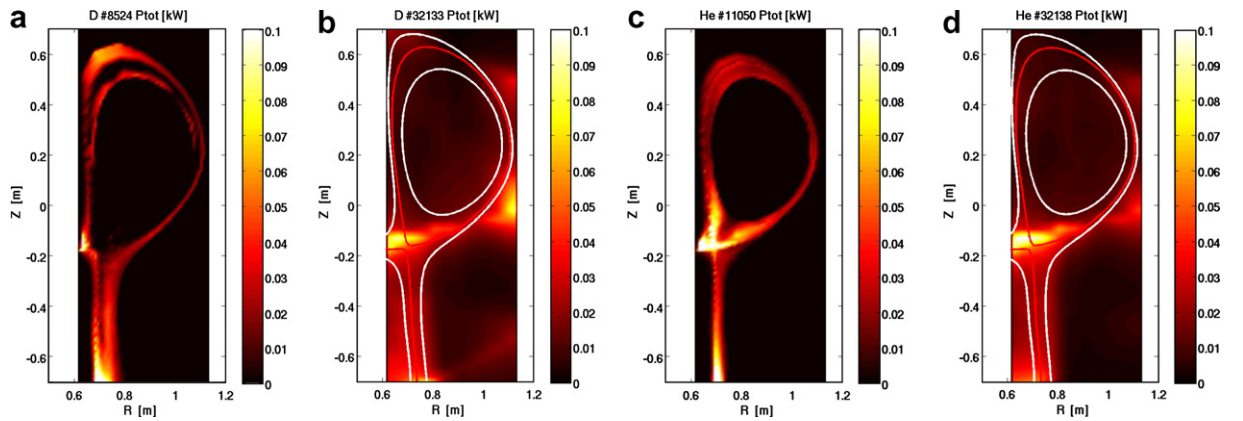

Fig. 4. Total radiative power distributions according to a SOLPS5 simulation: (a) and (c) and according to a tomographic image of foil bolometer signals, (b) and (d) for low density D and He discharges, respectively. The numbers correspond to the power emitted by a given poloidal area integrated over its toroidal volume. The area enclosed by the two white lines is covered by the SOLPS5 simulation. Red line – the separatrix. (For interpretation of the references in color in this figure legend, the reader is referred to the web version of this article.)

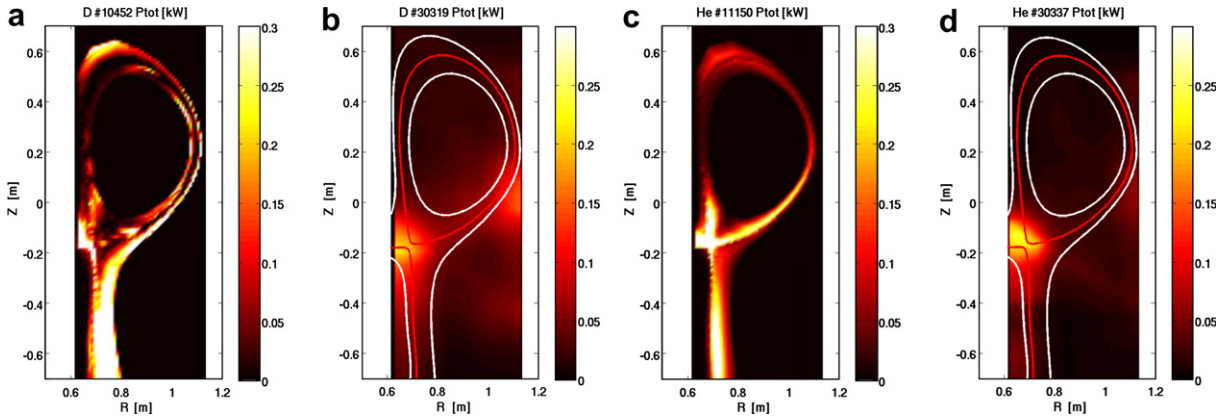

Fig. 5. Same as Fig. 4 but for the high density D and He discharges.

sources around the low field side (LFS) midplane region. Unfortunately the bolometer chord coverage (there are no sight lines crossing the LFS main chamber wall other than those belonging to the cameras mounted on the outboard lateral ports, see Fig. 1) does not permit detailed resolution in this region. In the absence of sufficient crossed chords the tomography procedure will always 'concentrate' the radiation into the regions, i.e. at the top right and middle lateral cameras. This fact was also checked with reconstructions of special phantom radiation distributions. However, the AXUV images also show a radiating zone on the LFS wall at the height of the magnetic axis, but in this case the reduced sensitivity prevents a detailed study. On possible explanation for these LFS radiation zones is an enhanced level of particle transport in the outboard midplane region. Such transport has recently been directly measured and quantified on TCV by comparing observations of the turbulent density and flux time series with predictions of a 2D fluid turbulence code [14]. Increased convective transport of this nature has in fact also been a necessary inclusion in the high density SOLPS5 simulations used here (see Fig. 5 and Table 1 cases #10841, #11150) in order to approach the levels of divertor detachment that are seen at the outer target at high density [12]. Such transport has potential for impurity release and should be more noticeable in D plasmas where the relatively low energy turbulent fluxes can more readily release C impurities through chemical sputtering. This appears to be the case when comparing the D and He reconstructions at high density in Fig. 5.

Table 1 summarizes the total radiative power measured and simulated for the three regions for low/high densities and He/D plasma species. At low densities the SOLPS5 power is rather well matched by foil bolometry power, but there is a substantial power generated by radiation outside the region covered by the simulation grid. This provides strong motivation to attempt to extend the simulation grid to the wall shadow regions in the longer

Table 1
The total radiated powers calculated for the three poloidal regions: range 1, 2 and 3

	SOLPS5 (kW)	FOIL (kW)	AXUV (kW)
Low density D (experiment #32133)			
SOLPS range (range 1, simulation #8524)	51.4	58.9	11.9
Inside SOLPS (range 2)		14.4	15.6
Outside SOLPS (range 3)		47.2	9.3
Low density He (experiment #32138)			
SOLPS range (range 1, simulation #11050)	51.0	59.9	22.61
Inside SOLPS (range 2)		12.2	19.4
Outside SOLPS (range 3)		36.4	14.3
High density D (experiment #30319)			
SOLPS range (range 1, simulation #10841)	376	123	27.0
Inside SOLPS (range 2)		40.1	47.3
Outside SOLPS (range 3)		117	32.4
High density He (experiment #30337)			
SOLPS range (range 1, simulation #11150)	158	95.8	35.4
Inside SOLPS (range 2)		24.1	27.9
Outside SOLPS (range 3)		76.2	25.0

For explanation see text.

term. At high densities in contrast, only the sum of the bolometer radiation inside and outside the code simulation domain is close to the predicted power. This might indicate that either some of the power assumed by SOLPS5 to be generated inside its grid area in fact is generated outside, or that SOLPS5 simply overestimates the power radiated in the simulated region. In addition to the convective transport, the code simulation case #10841 was performed using an artificially enhanced Y_{chem} at the main chamber wall of 10% in order to produce the observed levels of divertor detachment [13]. Moreover, the enhanced Y_{chem} was assumed to be poloidally uniform. In the He case, the power accounting is improved, providing further evidence that the discrepancy at high density is linked to the way in which impurity release is simulated.

Comparing the foil and AXUV bolometry derived total radiation, both are well matched at all densities and for both He and D only for the central, confined plasma region, but not elsewhere. This is a direct further evidence for the combined effect of diode ageing and reduced response at low energies. It is remarkable though, that the ratios of foil and AXUV powers in the inside and outside domains are rather constant and seem to be only the functions of the main plasma species. The ratio is around 4.5–5 for D and around 2.5–3 for He. This fact might open a possibility to correct for the reduced AXUV responsivity at low energies if calibrated against foil bolometers for different plasma scenarios.

Acknowledgement

This work was supported in part by the Swiss National Science Foundation and EURATOM.

References

[1] K. McCormick, A. Huber, C. Ingesson, et al., Fus. Eng. Des. 74 (2005) 679.
[2] R.L. Boivin, J.A. Goetz, E.S. Marmar, et al., Rev. Sci. Instrum. 70 (1999) 260.
[3] D.S. Gray, S.C. Luckhardt, L. Chousal, et al., Rev. Sci. Instrum. 75 (2004) 376.
[4] C. Suzuki, B.J. Peterson, K. Ida, Rev. Sci. Instrum. 75 (2004) 4142.
[5] A.W. Leonard, M.A. Mahdavi, S.L. Allen, et al., Phys. Rev. Lett. 78 (1997) 4769.
[6] <http://www.ird-inc.com>.
[7] <http://www-cfadc.phy.ornl.gov/adas/adas.html>.
[8] I. Furno, H. Weisen, J. Mlynar, et al., Rev. Sci. Instrum. 70 (1999) 4552.
[9] A.W. Degeling, H. Weisen, A. Zabolotsky, et al., Rev. Sci. Instrum. 75 (2004) 4139.
[10] M. Anton, H. Weisen, M.J. Dutch, et al., Plasma Phys. Control. Fus. 38 (1996) 1849.
[11] R. Schneider, X. Bonnin, K. Borrass, et al., Contribution Plasma Phys. 46 (2006) 3.
[12] M. Wischmeier, R.A. Pitts, J. Horacek et al., in: 32nd EPS Conference on Plasma Physics, Tarragona, 27 June–1 July 2005 ECA, vol. 29C, 2005, P-5.013.
[13] M. Wischmeier, Simulating divertor detachment in the TCV and JET tokamaks, PhD thesis in CRPP report LRP 799/05, 2005.
[14] O.E. Garcia, J. Horacek, R.A. Pitts, et al., Plasma Phys. Control. Fus. 48 (2006) L1.